VI. NUCLEAR MAGNETIC RESONANCE AND HYPERFINE STRUCTURE

Prof. F. Bitter
Prof. L. C. Bradley III
Prof. J. S. Waugh
Dr. P. C. Brot
Dr. H. H. Stroke
Dr. J. F. Waymouth
R. L. Fork
H. R. Hirsch
R. J. Hull
C. S. Johnson, Jr.
R. H. Kohler
Ilana Levitan
J. H. Loehlin
F. Mannis
I. G. McWilliams
P. G. Mennitt
S. R. Miller
E. C. Penski
C. J. Schuler, Jr.
W. W. Smith
C. V. Stager
W. T. Walter
S. T. Wray, Jr.

A. MACHINE CALCULATION OF NUCLEAR RESONANCE SPECTRA

The usual method of determining the chemical shifts and spin-spin coupling constants that are responsible for the high-resolution nuclear magnetic-resonance spectrum of a molecule is basically iterative: A trial set of these parameters is assumed, the spin Hamiltonian diagonalized numerically, and the input parameters modified on the basis of a comparison of the result with the experimentally determined spectrum. The only steps in this procedure that are most efficiently performed by a human operator are the comparison of computed results with experiment and the subsequent choice of modified input parameters. In collaboration with Dr. A. A. Bothner-By and Dr. C. Saalbach, of the Mellon Institute, an IBM 704 program has been developed, in which the spectrum for a given set of parameters is calculated and displayed on an oscilloscope screen. The operator controls the input to the computer with a Flexowriter keyboard. This work is being done under the auspices of the Computation Center, M.I.T.

C. S. Johnson, Jr.

B. SPIN-LATTICE RELAXATION OF I^{127} IN VARIOUS CHEMICAL ENVIRONMENTS

In connection with the design of an experiment to observe pure quadrupole resonance in liquids whose molecules are partially aligned in an electric field, the relaxation times of I^{127} nuclei in a number of different chemical media are being measured. The relaxation time is an extremely sensitive indicator of the degree of chemical association (departure from average spherical symmetry) of the iodine in a solution. The equilibrium and chemical exchange rate properties of I^-, I_2, and I_3^- are being studied at present.

F. Mannis

C. HYPERFINE STRUCTURE OF Hg^{197}: AN APPLICATION OF THE LEVEL-CROSSING TECHNIQUE

Colegrove, Franken, Lewis, and Sands (1) have reported a novel spectroscopic method of measuring the fine structure of the $2\ ^3P$ state in helium. This method depends on the interference of probability amplitudes in two degenerate Zeeman levels. They

suggested that a similar experiment could be used in other elements to study hyperfine structure.

We applied their technique to the measurement of the hyperfine structure of the $6\,^3P_1$ state in Hg^{197}. The apparatus was used by Hirsch for Zeeman-effect magnetic-scanning experiments (see Sec. VI-D) and for a level-crossing experiment (2) in Hg^{199}. The lamp, scanning magnet, quarter-wave plate, and polarizer constitute a variable-frequency source that can be set to excite the mercury atoms in the cell with light of approximately 2537 A wavelength. Two photomultipliers serve as monitors – one for the direct output of the lamp and one for the light scattered from the cell in the direction perpendicular to the incoming light and the splitting field. Their signals are combined in the photomultipler bridge in such a way that lamp fluctuations do not produce false peaks in the graph of scattered light versus splitting field that is produced by the recorder.

With the use of Melissinos' data (3), the splitting field was predicted to be 7417 gauss at the sole level crossing in Hg^{197}. The scanning field required to illuminate the atoms with the use of an Hg^{198} lamp was estimated to be 2200 gauss, with the quarter-wave plate and polarizer set so that only the lower-frequency Zeeman component of the lamp can pass through.

The quarter-wave plate and polarizer are positioned in such a way that the cell receives σ illumination because theory and experiment agree that this produces the best signal-to-noise ratio when the incoming light is perpendicular to the splitting field. With the splitting field set at 7417 gauss, the scanning field is varied around 2200 gauss until the scattered light is maximized. This occurs at 2420 gauss. The photomultiplier bridge is balanced to make maximum scattered light correspond to zero reading on the recorder, and the splitting field is swept in the vicinity of 7400 gauss. At 7401.0 gauss, as measured by a proton resonance magnetometer, there is a sudden dip in scattered light intensity corresponding to an intersection of levels in the Zeeman pattern of Hg^{197}. The width of the dip at half-depth is 2 gauss, a figure typical of the natural linewidths of the levels. A signal-to-noise ratio of approximately 10 is obtained with an amplifier bandwidth of approximately one cycle per second.

The use of degenerate-state perturbation theory yields the relation between the splitting field, H_+, at which two levels cross, and the magnetic dipole interaction constant, A. The Hamiltonian is

$$\mathcal{H} = A\vec{I}\cdot\vec{J} - \vec{\mu}_T\cdot\vec{H}$$

where $\vec{\mu}_T$ is the total magnetic moment of the atom, and $\vec{I}$ and $\vec{J}$ are the nuclear and electronic angular moments, respectively, measured in units of $\hbar$. If H, the magnetic field, is taken in the z-direction, the Hamiltonian becomes

$$\mathcal{H} = A\vec{I}\cdot\vec{J} + g\mu_o H J_z - g_I r\mu_o H I_z$$

where r is the electron-to-proton-mass ratio, μ_o is the Bohr magneton, and g and g_I are the electron and proton g-factors, respectively. Matrix elements of $\mathscr{H}$ are calculated in the I, J, F, m_F representation for J = 1, I = 1/2; this gives matrices of $\mathscr{H}$ that are diagonal in m_F. The m_F = 1/2 matrix is 2 × 2 and, when it is diagonalized, yields the equation of the F = 1/2, m_F = 1/2 level as a function of H. The F = 3/2, m_F = -3/2 level is linear in H, coming directly from a "1 × 1 matrix." A is found by setting the energies of these levels equal.

$$A = g\mu_o H_+ \frac{1 - \frac{g_I}{g} r}{1 - \frac{1}{2}\frac{g_I}{g} r} \tag{1}$$

The quotient on the right-hand side differs from unity by approximately one part in 11,000 for Hg^{197}. The difference is not important for the rest of the calculations in this report, and hence will be neglected, so that the simple equation

$$A = g\mu_o H_+ \tag{2}$$

remains.

Knowing H_+, the accuracy with which we can find A is limited by the accuracy with which g is known. According to Brossel and Bitter (4), g = 1.4838 ± .0004 in the $^3P_1$ state of mercury. H_+ has been measured six times with a standard deviation, σ, of a part in 19,000. This is with reference to the field at the position of the magnetometer probe. The field in the cell is approximately 2.7 gauss higher, and is known with less precision, since it cannot be measured at the time a level crossing is observed. Using these figures, we find that A = 15,377 ± 15 mc. The tolerance is simply a conservative estimate, and is not the result of a statistical analysis.

The A values of Hg^{197} and Hg^{199} differ by less than 5 per cent. Thus, in taking ratios of these A values, the probe-to-cell distance correction is reduced by a factor of 20 to negligible proportions, the g-factor drops out entirely, and we have

$$\frac{A_{197}}{A_{199}} = \frac{H_{+197}}{H_{+199}} \tag{3}$$

where H_+ can now be taken at the position of the proton-resonance probe. H_+ was measured six times for Hg^{199}, and six A-value ratios were computed. Their average, A_{197}/A_{199}, is 1.04315 with a standard deviation of 9.6×10^{-5}. Stager (5) has determined A_{199} = 14,752.37 ± .02 mc. Using this figure, and taking 3σ limits as tolerances, we have A_{197} = 15,388.9 ± 4.5 mc. This is to be compared with Melissinos' (3) value of 15,405 ± 30 mc. The zero-field separation between the Hg^{197} F = 3/2 and F = 1/2 levels is 3/2 A_{197}, or 23,083.4 ± 6.7 mc.

H. R. Hirsch, C. V. Stager

References

1. F. D. Colegrove, T. A. Franken, R. R. Lewis, and R. H. Sands, Novel method of spectroscopy with applications to precision fine structure measurements, Phys. Rev. Letters 3, 420 (1959).

2. H. R. Hirsch, Hyperfine structure of Hg^{199} – An application of the level-crossing technique, a paper submitted for the American Physical Society Washington Meeting, April 25-28, 1960.

3. A. C. Melissinos, Determination of the Dipole Moment and Isotope Shift of Radioactive Hg^{197} by "Double Resonance," Technical Report 346, Research Laboratory of Electronics, M.I.T., Nov. 10, 1958; Phys. Rev. 115, 126-129 (1959).

4. J. Brossel and F. Bitter, A new "double-resonance" method for investigating atomic energy levels – Application to Hg $^3P_1$, Phys. Rev. 86, 308-316 (1952).

5. C. V. Stager, Hyperfine structure of Hg^{199} and Hg^{201} in the $^3P_1$ state, a paper submitted for the American Physical Society Washington Meeting, April 25-28, 1960.

D. PHOTOMULTIPLIER BRIDGE FOR MAGNETIC-SCANNING EXPERIMENTS

In magnetic-scanning experiments on mercury (1), the intensity of light scattered by the vapor in the cell is the variable under study. The signal photomultiplier is illuminated by this light, and, inevitably, by background light reflected from the walls of the cell. Thus lamp intensity variations (see Section VI-E) will distort the base line of the signal photomultiplier current, and thus make the observation of scanning peaks tedious and difficult.

Accordingly, the experimental arrangement of Fig. VI-1 has been devised. The outputs of the signal and lamp photomultipliers are combined in a bridge circuit which, if it operated ideally, would yield a flat base line on the recorder chart, regardless of lamp intensity. The presence of a peak would indicate scattering of light by the mercury vapor. Since the bridge measures the difference between the photomultiplier currents, rather than their ratios, it does not remove the effect of intensity changes on scanning peak heights.

To use the bridge, the detector (2) and relay must be set in phase by adjusting the phase shifter to give a maximum recorder reading. In order to achieve a balance, the mercury vapor is removed from the body of the cell by dipping its tail in liquid nitrogen. Then the resistance, R, is varied to obtain a zero recorder indication. After the liquid nitrogen is replaced by iced water, the balance is maintained unless the mercury itself is scattering light.

The mercury reed relay alternately connects each photomultiplier voltage to the grid of the electrometer tube. The tube's ac output, proportional to the difference of these voltages, is amplified, rectified by the phase detector, and displayed on the chart

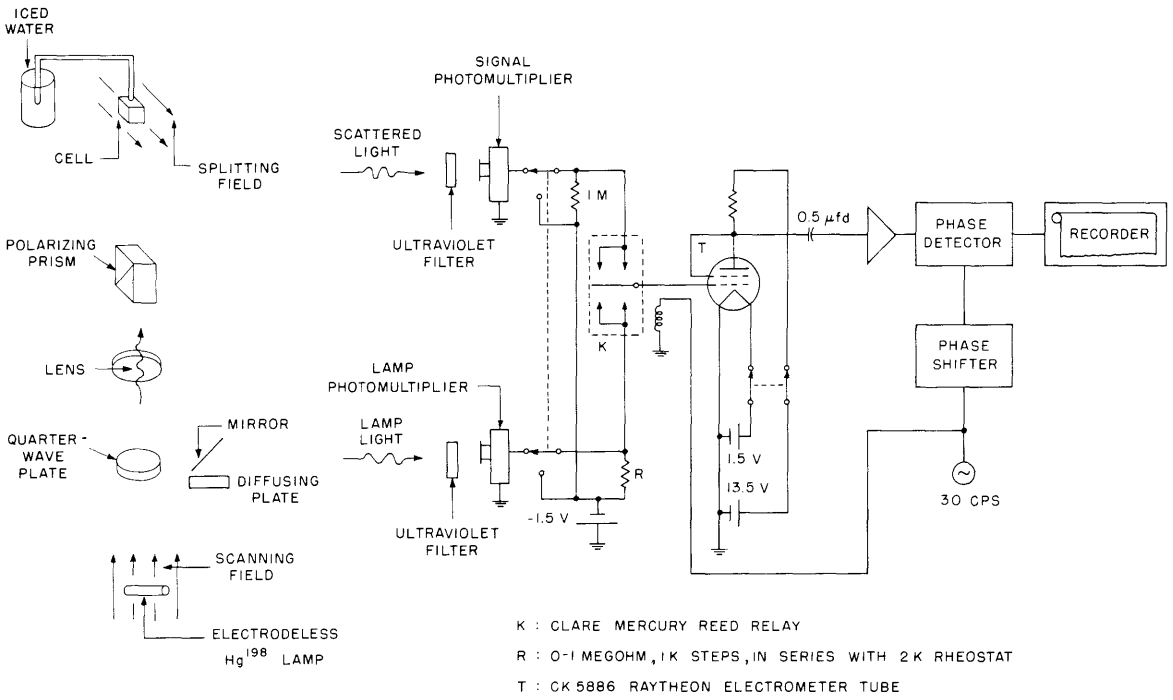

Fig. VI-1. Diagram of apparatus for magnetic-scanning experiments.

recorder. The advantage of this arrangement is that no matched amplifier units are required. The electrometer tube is used because the fraction of a microampere of grid current in an ordinary tube is of the same order of magnitude as the current from the signal photomultiplier, and is sufficient to upset the balance.

The fused-quartz diffusion plate and front-surfaced mirror make it possible to locate the lamp photomultiplier far enough from the scanning magnet so that it will not be seriously affected by stray fields. At this distance, if the diffusing plate were not used, only part of the electrodeless discharge lamp would illuminate the phototube, and, since the discharge shifts position inside the lamp, the bridge would be virtually worthless.

In practice, the bridge reduces base-line fluctuations by a factor of 10, at least. This has proved adequate for obtaining natural and radioactive mercury scanning curves.

H. R. Hirsch

References

1. F. Bitter, S. P. Davis, B. Richter, and J. E. R. Young, Phys. Rev. 96, 1531 (1954).

2. For a complete description of the phase detector, phase shifter, and 30-cycle source, see G. R. Murray, Jr., Molecular Motions in Crystals: A Nuclear Resonance Investigation of the Hexamminecobalt (III) Salts, Ph.D. Thesis, Department of Chemistry, M.I.T., 1956.

E. INTENSITY AND LINEWIDTH OF AN ELECTRODELESS DISCHARGE LAMP IN A MAGNETIC FIELD

The intensity of a water-cooled electrodeless discharge lamp (1) containing Hg^{198} has been measured as a function of magnetic field. The field in a direction perpendicular to the lamp's axis was cycled ±15,000 gauss for a number of times. After the first quarter-cycle, starting from zero field, a fairly reproducible intensity versus field plot (Fig. VI-2) was obtained as the field went from the positive to negative direction, and an entirely different, fairly reproducible plot (Fig. VI-3) was obtained in the negative-to-positive direction. In both cases, the intensity dropped at high field strengths. In a magnetic-scanning experiment, the lamp displayed a Doppler width of 2000 mc.

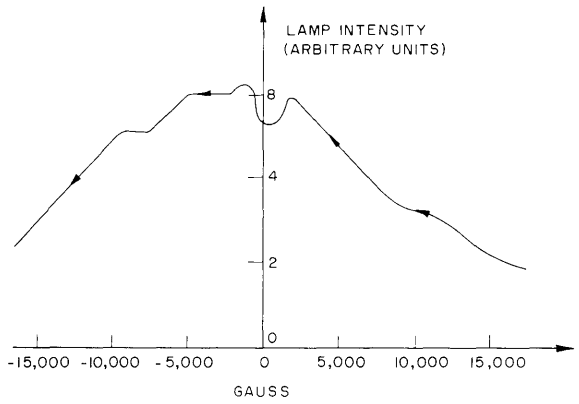

Fig. VI-2. Graph of light intensity for magnetic-field change from the positive to the negative direction.

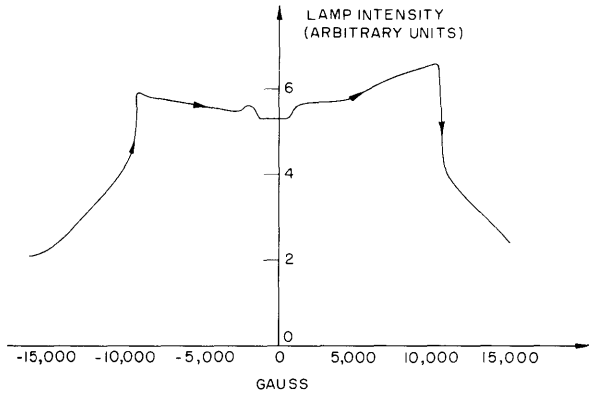

Fig. VI-3. Graph of light intensity for magnetic-field change from the negative to the positive direction.

This behavior is to be contrasted with that observed by Melissinos (2) in a similar lamp cooled by dry nitrogen blast. He found that the temperature and intensity rose in sharp steps toward high magnetic fields. He also noticed that his curves were different in the different directions of field travel, although they resembled each other more than the curves for the water-cooled lamp do. The gas-cooled lamp showed a Doppler linewidth of 3500 mc.

H. R. Hirsch

References

1. H. R. Hirsch, Water-cooled electrodeless mercury-discharge lamp, Quarterly Progress Report No. 55, Research Laboratory of Electronics, M.I.T., Oct. 15, 1959, p. 68.

2. A. C. Melissinos, The Magnetic Dipole Moment and Isotope Shift of Hg^{197}, Ph.D. Thesis, Department of Physics, M.I.T., 1958.

F. HYPERFINE STRUCTURE OF THE $^3P_1$ STATE OF Hg^{199}

The transition between the F = 1/2 → F = 3/2 levels of the 6 $^3P_1$ state of Hg^{199} has been previously reported (1). The preliminary data were for the $\left(F = \frac{3}{2}, M_F = -\frac{3}{2}\right) \leftrightarrow \left(F = \frac{1}{2}, M_F = -\frac{1}{2}\right)$ transition. The frequency was obtained as a function of magnetic field (5-20 gauss) and extrapolated to zero field.

To improve the signal-to-noise ratio, the bandwidth of the detector was decreased. A further improvement in signal-to-noise ratio was achieved by using $\left(\frac{3}{2}, -\frac{3}{2}\right) \leftrightarrow \left(\frac{1}{2}, -\frac{1}{2}\right)$ and $\left(\frac{3}{2}, \frac{1}{2}\right) \leftrightarrow \left(\frac{1}{2}, \frac{1}{2}\right)$ transitions for frequencies lower than the zero-field value. These transitions would be degenerate if the nucleus had zero magnetic moment. Because of the short lifetime of the $^3P_1$ state (1.2×10^{-7} sec), the natural linewidth made it impossible to resolve them. For frequencies higher than the zero field value, the $\left(\frac{3}{2}, -\frac{1}{2}\right) \leftrightarrow \left(\frac{1}{2}, -\frac{1}{2}\right)$ and $\left(\frac{3}{2}, \frac{3}{2}\right) \leftrightarrow \left(\frac{1}{2}, \frac{1}{2}\right)$ transitions were used.

The deviations from the linear Zeeman effect were estimated by first-order perturbation theory and the zero-field splitting was obtained by a least-square fit.

The experimental value for the 6 $^3P_1$ splitting in Hg^{199} is 22,128.56 ± .02 mc. The error is the probable error obtained from the least-square fit.

C. V. Stager

References

1. C. V. Stager, Hyperfine structure of the $^3P_1$ state of mercury by double-resonance methods, Quarterly Progress Report No. 56, Research Laboratory of Electronics, M.I.T., Jan. 15, 1960, p. 92.

G. NUCLEAR ORIENTATION BY OPTICAL PUMPING

1. Introduction

Optical pumping in mercury vapor, resulting in a two-to-one population ratio of the ground sublevels of Hg^{199}, has been achieved. A variable-frequency light source was used to illuminate a cell containing the Hg^{199} vapor. The theoretical considerations leading to this result will be reported here, and the experimental work will be described in a later report.

An optical-pumping experiment was set up in the Magnet Laboratory to orient Hg^{199} nuclei in the m = +1/2 magnetic ground sublevel. A cell containing Hg^{199} vapor is illuminated only by the right circularly polarized component σ^+ of the 2537 A mercury resonance line. Then, as shown in Fig. VI-4 (reproduced from Brossel and Bitter (1)), atoms in the m = -1/2 ground sublevel absorb the 2537 A σ^+ radiation going to the m = +1/2, F = 1/2 sublevel of the $^3P_1$ excited level [lifetime $\tau = 1.18 \times 10^{-7}$ sec (2)]. The m = +1/2 ground sublevel does not absorb the σ^+ light. When the atoms return to the ground state, two-thirds of them re-emit the σ^+ radiation and return to the m = -1/2 sublevel; but one-third emit π radiation and go to the m = +1/2 ground sublevel. Thus, as this process continues, all of the atoms would be "pumped" into the m = +1/2 ground sublevel if there were no disorientation processes.

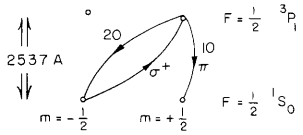

Fig. VI-4. Resonance radiation of the 2537 A line in Hg^{199} (I=1/2) with transition probabilities indicated.

Collisions with other atoms in the vapor, collisions with the walls of the cell, and condensation of the Hg^{199} vapor are possible causes of disorientation. These disorienting mechanisms create a relaxation process that competes with the pumping process and tends to restore equal ground sublevel populations. (The Boltzmann thermal population difference caused by the small energy difference between the ground sublevels is neglected here because the population difference obtained by optical pumping is more than a million times greater.) The time constants of these two competing processes, τ_P of the pumping process and τ_R of the relaxation process, and the steady-state value of the ratio α of the ground sublevel populations will be derived. Computations have been made specifically for the experimental apparatus in the Magnet Laboratory to orient Hg^{199}.

2. Theory

The situation that will be considered consists of a cell containing Hg^{199} vapor which is illuminated only by the σ^+ component of the 2537 A resonance line of the vapor. To keep collisions involving Hg^{199} to a minimum, no buffer gas is included in the cell. The

assumptions, then, are that the effects from σ^- light or π light, as well as other atoms than Hg^{199} in the cell, may be neglected.

At the vapor pressures ($P < 10^{-4}$ mm Hg) and with the cell dimensions ($a > 2$ cm) used, collisions between mercury atoms are a thousand times less frequent than collisions with the walls. Moreover, the most likely ground-level mercury-mercury collisions that change nuclear orientation are those resulting in an exchange of spins between the two nuclei. These do not change either ground sublevel's population in the vapor. On this basis, the destruction of orientation caused by mercury-mercury collisions will be neglected as compared with mercury-cell wall collisions. Collisions with the walls and condensation of the vapor in the cell are therefore assumed to be the disorienting mechanisms giving rise to a relaxation process.

The following ground-level orientation-producing and orientation-destroying mean times are defined as

$\tau_A \equiv$ mean time required for an Hg^{199} atom in the m = -1/2 ground sublevel to absorb a 2537 A σ^+ photon;

$\tau_w \equiv$ mean time required for an Hg^{199} atom in the cell to make a wall collision;

$\tau_c \equiv$ mean time required for an Hg^{199} atom in the cell to condense in the cooled portion of the cell's tail.

The photon-absorption, wall-collision, and condensation rates are the reciprocals of τ_A, τ_w, and τ_c, respectively.

The following definitions will also be used:

$n_o \equiv$ density of Hg^{199} atoms in the vapor in the cell;

$n \equiv$ density of Hg^{199} atoms in the m = +1/2 ground sublevel;

$\alpha \equiv \frac{n}{n_o - n}$ = equilibrium ratio of the ground sublevel populations ($1 < \alpha < \infty$);

$\beta \equiv$ fraction of wall collisions that are disorienting ($0 < \beta < 1$).

Now, the increase in density of Hg^{199} atoms in the m = +1/2 ground sublevel per second, dn/dt, is equal to the density of the Hg^{199} atoms in the -1/2 ground sublevel ($n_o - n$) times the rates transferring them to the +1/2 ground sublevel, minus the density of Hg^{199} atoms already in the +1/2 ground sublevel times the rates transferring them back. Therefore

$$\frac{dn}{dt} = (n_o - n)\left[\frac{1}{3}\tau_A^{-1} + \beta\tau_w^{-1} + \frac{1}{2}\tau_c^{-1}\right] - n\left[\beta\tau_w^{-1} + \frac{1}{2}\tau_c^{-1}\right]$$

Here, it is assumed that following condensation, evaporation to the m = -1/2 and m = +1/2 ground sublevels is equally probable.

Steady state is reached when dn/dt = 0, and thus

$$\alpha \equiv \frac{n}{n_o - n} = 1 + \frac{1}{3\tau_A\left(\frac{\beta}{\tau_w} + \frac{1}{2\tau_c}\right)} \qquad (1)$$

The equilibrium ground sublevel ratio a varies from 1 (no orientation) to ∞ (complete orientation). The percentage of optical pumping is $100\,\frac{a-1}{a+1}$. The solution of the differential equation governing the pumping

$$\frac{dn}{dt} + \left(\frac{1}{3\tau_A} + \frac{2\beta}{\tau_w} + \frac{1}{\tau_c}\right)n = \left(\frac{1}{3\tau_A} + \frac{\beta}{\tau_w} + \frac{1}{2\tau_c}\right)n_o \tag{2}$$

is

$$n = \frac{n_o}{a+1}\left[a - \frac{1}{2}(a-1)\,e^{-t/\tau_P}\right] \tag{3}$$

where the optical-pumping time constant τ_P, the mean time required for the Hg^{199} atom to be optically pumped, is given by

$$\tau_P \equiv \frac{1}{\frac{1}{3\tau_A} + \frac{2\beta}{\tau_w} + \frac{1}{\tau_c}} \tag{4}$$

The Boltzmann difference has been neglected here, and equal populations $n_o/2$ have been assigned to each magnetic sublevel at t = 0.

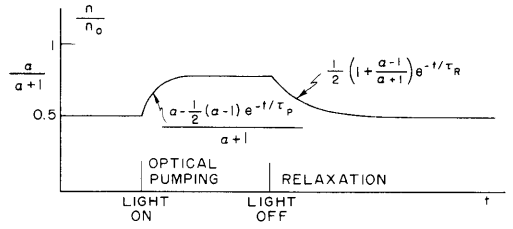

Fig. VI-5. Population changes of Hg^{199} m = +1/2 ground sublevel.

When the steady-state oriented population has been reached, if the light is turned off, the ground sublevel populations will equalize. The governing equation is

$$n = \frac{n_o}{2}\left[1 + \frac{a-1}{a+1}\,e^{-t/\tau_R}\right] \tag{5}$$

where the relaxation time constant τ_R is given by

$$\tau_R \equiv \frac{1}{\frac{2\beta}{\tau_w} + \frac{1}{\tau_c}} \tag{6}$$

We may also express a in terms of τ_P and τ_R.

$$\alpha = 2\frac{\tau_R}{\tau_P} - 1 \tag{7}$$

Figure VI-5 illustrates these results.

3. Apparatus and Experiments

The apparatus is shown in Fig. VI-6. A variable-frequency light source is obtained by placing an Hg^{198} lamp in a 4-inch Bitter solenoid which provides a strong magnetic field ($H_L \equiv$ scanning field < 30,000 gauss). The wavelength of the light used to illuminate the cell can then be varied 0.12 A on either side of the 2536.51 A zero-field line of Hg^{198}. The cell containing the Hg^{199} vapor is placed in the center of a set of Helmholtz coils that provide a weak magnetic field ($H_o \equiv$ splitting field < 1000 gauss).

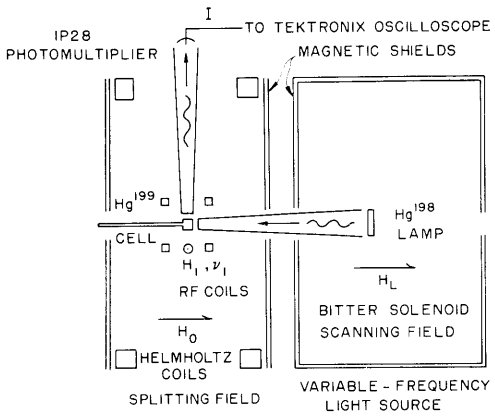

Fig. VI-6. Top view of apparatus.

A scanning field of 7100 gauss will Zeeman-shift the 2537 A σ^+ component of Hg^{198} resonance radiation so that it will coincide with the Hg^{199} 2537 A resonance transition to the $F = 1/2$, $^3P_1$ level. The σ^- component that is Zeeman-shifted in the other direction will pass unabsorbed through the cell's vapor because it does not overlap any Hg^{199} transition. Optical pumping will then take place in the cell in accordance with Eq. 3. The intensity of the light reradiated from the cell perpendicular to the incident 2537 A σ^+ radiation will be proportional to the $m = -1/2$ ground sublevel population. Therefore

$$I = \frac{I_o}{\alpha + 1}\left[2+(\alpha-1)\, e^{-t/\tau_P}\right] \tag{8}$$

where I_o is the intensity reradiated when half of the cell's Hg^{199} atoms are in the $m = -1/2$ ground sublevel (t=0).

It should be noted that neither polarizer nor analyzer need be inserted in the incident or scattered light beams in this experimental arrangement. The scanning field acts as a polarizer; and an analyzer is not necessary whenever optical pumping is performed through an excited level having the same F value as the ground level, so that the transparency of the vapor with respect to the incident σ^+ light increases with pumping.

If H_L has been set at 7100 gauss and the splitting field is turned on so that H_o

is parallel to H_L, then, when the lamp is turned on, the photomultiplier current, which is proportional to I, should decay as indicated in Fig. VI-7. From such a curve both a and τ_P can be determined. With these two values, τ_R and τ_A can be determined from Eqs. 4, 6, and 7.

$$\tau_R = \frac{1}{2}\tau_P(a+1) \tag{9}$$

$$\tau_A = \frac{1}{3}\tau_P\frac{a+1}{a-1} \tag{10}$$

Under assumptions (i) and (ii), which will be discussed in section 4, the condensation time constant τ_c can be measured by placing the tail of the cell in liquid air and determining the time constant of the resulting decrease in photomultiplier current. If the kinetic-theory estimate is taken for τ_w, then the disorienting fraction of wall collisions can be determined from Eq. 7.

$$\beta = \frac{1}{2}\tau_w\left(\frac{1}{\tau_R} - \frac{1}{\tau_c}\right) \tag{11}$$

Since a, τ_P, and τ_R are related through Eq. 7, an experimental measure of all three would yield an estimate of the adequacy of the theory developed in this paper. The quantities a and τ_P can be determined from an oscilloscope trace similar to that shown in Fig. VI-7 which could be made by quickly opening a shutter between the lamp and the cell. Although the vapor relaxes in the dark, it is still possible to plot the relaxation curve on an oscilloscope by Franzen's method (3) and determine the time constant τ_R. If, after the vapor has reached its steady-state oriented value, the shutter between the lamp and cell is closed and the time before reopening it is varied, then the points from which the pumping exponential begins will plot the relaxation exponential as indicated in Fig. VI-8.

Advantage may be taken of the population difference created by optical pumping in a

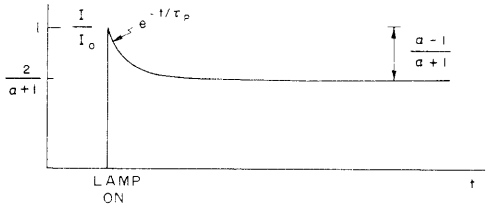

Fig. VI-7. Phototube current with the optical-pumping exponential shown.

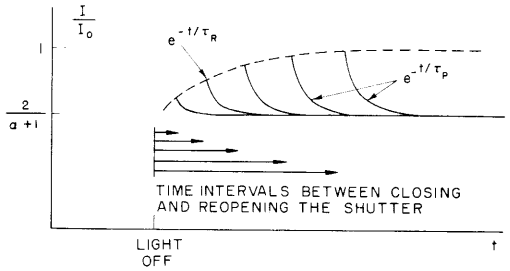

Fig. VI-8. Phototube current with the relaxation exponential shown.

more important experiment, the determination of the energy difference between the ground sublevels at a known splitting field H_o. This would yield the nuclear g-value, and hence the magnetic moment of Hg^{199}, since the nuclear spin is known to be 1/2. If H_o is held at an accurately known value, then the frequency applied to a set of rf coils about the cell, which causes the photomultiplier current to return to I_o, is the resonance frequency ν_1 that corresponds to an energy difference of $h\nu_1$ between the Hg^{199} ground sublevels. Then

$$\nu_1 = g \frac{e}{4\pi M_P c} H_o \tag{12}$$

where M_P is the mass of the proton.

4. Kinetic Theory Determination of τ_A, τ_w, and τ_c

We shall now use kinetic-theory considerations of Hg^{199} collisions with 2537 A σ^+ photons, with the cell walls, and with condensed Hg^{199} to determine the time constants τ_A, τ_w, and τ_c in terms of the lamp intensity, experimental dimensions, and physical constants.

Consider a point 2537 A σ^+ photon moving in a volume containing stationary $\left[\frac{\text{photon speed}}{\text{atom speed}} \approx 10^6\right]$ Hg^{199} atoms that have a cross-section area (σ_A) of absorption for this resonance photon. When the mercury atoms are so far apart that their absorption cross sections do not screen each other, then the absorption area that the photon sees per centimeter of path is just the number of mercury atoms in this centimeter slice of vapor multiplied by the absorption cross section σ_A of an atom. The probability of a photon being absorbed per centimeter of path is the ratio of this absorption area to the cross-section area containing the mercury atoms. Therefore the number of absorptions per 2537 A σ^+ photon per centimeter of photon path is $(n_o - n)\,\sigma_A$.

$$\text{Number of absorptions/photon-cm} = (n_o - n)\,\sigma_A = \frac{\phi_R}{\phi_c} \tag{13}$$

in which the following definitions have been used to set up the second expression:

$\phi_c \equiv$ number of 2537 A σ^+ photons entering the cell per square centimeter per second;

$\phi_R \equiv$ number of 2537 A photons absorbed and reradiated per cubic centimeter per second in the cell.

Now, the number of absorptions per second per Hg^{199} atom in the m = -1/2 ground sublevel is $\phi_c \sigma_A$. Hence the mean time for this mercury atom to absorb the 2537 A σ^+ photon is

$$\tau_A = \frac{1}{\phi_c \sigma_A} \tag{14}$$

If ϕ_L represents the number of 2537 A σ^+ photons per square centimeter per steradian per second leaving the lamp, A represents the emitting area of the lamp, and d is the lamp-to-cell distance, then

$$\phi_c = \frac{\phi_L A}{d^2} \tag{15}$$

The absorption cross section of an atom for its resonance radiation can be derived from Planck's black-body radiation law (4). When this is done by replacing the absorption line with a square line shape whose height is equal to the maximum absorption at the center of the line, and whose width is so determined that the area under the square line shape is equal to that under a Doppler-broadened absorption line, then the absorption cross section is given by

$$\sigma_A = 2\pi(\pi \ln 2)^{1/2} \lambda\!\!\!^{-2} \frac{g_2}{g_1} \frac{\Delta\nu_N}{\Delta\nu_D}$$

or

$$\sigma_A = 2\pi\left(\frac{\pi M}{8NkT}\right)^{1/2} \frac{\lambda\!\!\!^{-3}}{\tau} \frac{g_2}{g_1} \tag{16}$$

Here $\lambda\!\!\!^{-}$ is the wavelength of the resonance photon divided by 2π, τ is the lifetime of the excited level, g_1 and g_2 are the statistical weights of the ground and excited sublevels, M is the molecular weight of the absorber, N is Avogadro's number, k is Boltzmann's constant, and T is the temperature of the vapor in the cell. Since $g_1 = g_2 = 1$ for σ^+ light when optical pumping is performed through an excited F = 1/2 level, we have

$$\tau_A = \frac{1}{2\pi}\left(\frac{8NkT}{\pi M}\right)^{1/2} \frac{d^2}{\phi_L A} \frac{\tau}{\lambda\!\!\!^{-3}} \tag{17}$$

The mean time between the Hg^{199} atom's collisions with the cell walls is $a/\bar{v}$, where a is the linear dimension of the cubical cell (a < mean free path $\approx$ 10 cm), and $\bar{v} = (8NkT/\pi M)^{1/2}$ is the mean velocity of the Hg^{199} atom. Thus

$$\tau_w = a\left(\frac{\pi M}{8NkT}\right)^{1/2} \tag{18}$$

The mean time for an Hg^{199} atom in the vapor to condense depends on the shape of the cell. The following assumptions will be made to evaluate this rate: (i) The only liquid Hg^{199} is in the tip of the cell's tail which has been cooled to at least 30°C below room temperature (the temperature of the rest of the cell). (ii) The only sticking collisions between the Hg^{199} vapor and the cell walls occur in the tip of the cell's tail. (iii) Whenever an Hg^{199} atom in the cell enters the tail it will continue to bounce down

the tail until it condenses in the tip. Thus the mean time for condensation is equivalent to the mean time required by an Hg^{199} atom to find its way out of the cell into the tail.

An Hg^{199} atom within the cell makes $1/\tau_w$ collisions with the walls per second. One-sixth of these collisions are against the cell face to which the tail is connected. Now, f may be taken as the probability that an atom that strikes this face enters the tail, if f is defined as the ratio of the cross-section area of the hole in this face to the area of the cell face. Hence the mean time for an Hg^{199} atom to enter the tail is $6\tau_w/f$, and therefore

$$\tau_c = \frac{6\tau_w}{f} = \frac{6a}{f}\left(\frac{\pi M}{8NkT}\right)^{1/2} \tag{19}$$

5. Optical-Pumping Criterion

With the substitution of the kinetic-theory results of section 4 in Eq. 1, α becomes

$$\alpha = 1 + \left[\frac{\pi^2}{12}\frac{M}{NkT}\frac{\phi_L A}{d^2}\frac{\lambda\!\!\!^{-3}}{\tau}\right]\frac{a}{\beta + f/12} \tag{20}$$

Optical pumping is complete when $\alpha = \infty$. The criterion for complete orientation is that

$$\frac{\phi_L A}{d^2}\frac{M}{NkT}\frac{\lambda\!\!\!^{-3}}{\tau}\frac{a}{\beta + f/12} \gg 1 \tag{21}$$

It is evident that for the largest orientation:

(a) Pumping should be to the short-lived level closest to the ground level (i.e., maximum $\lambda\!\!\!^{-3}/\tau$).

(b) The brightest possible source of resonance radiation should be used as close as possible to the cell (i.e., maximum $\phi_L A/d^2$).

(c) The largest possible cell should be used (i.e., maximum a). However, consideration must be given to the homogeneity of the splitting field within the cell if an rf ground sublevel resonance ν_1 is to be performed.

(d) β and f should be made as small as possible. The hole connecting the tail to the cell should be designed to make $f \leq \beta$. Then the disorienting wall collisions will be the limiting relaxation factor, and will determine the amount of optical pumping that is

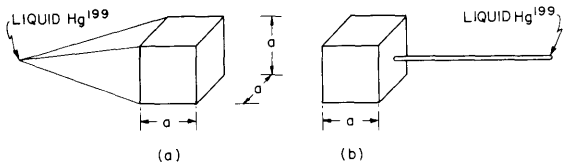

Fig. VI-9. Cells used in optical pumping: (a) original cell; (b) new cell.

possible. The original cells (see Fig. VI-9) used had f = 1, and so disorientation predominated because of condensation. Atoms in the vapor condensed before a significant population difference could be reached. This is the reason for the negative optical-pumping results obtained here, as Brossel (5) has pointed out. According to the calculations that will be given in section 6, less than 0.04 per cent of the atoms in the lower sublevel would be optically pumped in the original cell. The new cells (see Fig. VI-9b) have f = 1/16,000 and lead, as will be shown, to 30 per cent optical pumping.

(e) Low temperatures should be used. (The temperature is usually determined by the vapor pressure that is necessary to provide the cell with sufficient atoms to furnish a strong signal to the detection apparatus.)

To compare optical pumping in different elements consideration must be given to the mass of the atom, as well as to condition (a). If the other parameters (strength of light source, lamp size, lamp-to-cell distance, disorienting fraction of wall collisions, and temperature) are the same for each element, greater orientation would be expected for the 1849 A mercury resonance line and the 5890-5896 A sodium D lines (see Table VI-1).

Table VI-1. Factors for comparison of optical pumping in different elements.

Line	Atom	τ (sec)	$\frac{\lambda^3}{\tau}$	$M\frac{\lambda^3}{\tau}$
2537 A	Hg^{199}	1.18×10^{-7}	1	1
1849 A	Hg^{199}	1.3×10^{-9}	35	35
2349 A	Be^{7}	1.37×10^{-9}	68	2.4
5890 A	Na^{23}	1.6×10^{-8}	92	11

Note: Except for the value $\tau = 1.18 \times 10^{-7}$ sec, which is reported by Boutron, Barrat, and Brossel (2), all values are taken from H. H. Landolt and R. Börnstein, Zahlenwerte, Vol. 1, Pt. 1, Atome und Ionen (Springer Verlag, Berlin, 1950), pp. 264-266.

The 1849 A mercury line is beyond the spectral-sensitive range of the 1P28 photomultiplier tube. Since more sensitive ultraviolet photomultipliers are now becoming available, it may be possible to try optical pumping in mercury by means of the 1849 A resonance line.

This analysis indicates that with the sodium D lines in the visible part of the spectrum and intense lamps available, it should be easier to obtain optical pumping in sodium vapor. Franzen, Dicke, Hawkins, Dehmelt, Carver, and others are working in this

area. The problem is that the fraction of disorienting wall collisions is much larger in sodium than in mercury. Some success in reducing β has been achieved by coating the cell walls with a long-chain molecule or by trapping the atoms in a buffer gas.

6. Estimate of Optical Pumping in Hg^{199}

The calculation of the time constants and population ratio for our Hg^{199} optical-pumping experiment will now be discussed. First, however, estimates of the lamp intensity, ϕ_L, and the fraction of disorienting wall collisions, β, must be made.

The Hg^{198} lamp has been constructed in a pancake shape so that the light-emitting area within the 4-inch Bitter solenoid will be as large as possible. The intensity of the lamp can be estimated from the mercury-arc intensity measurements of Melissinos (6). The measured intensities of the 10 mercury lamps reported vary between 1 and 30 milliwatts per square centimeter per steradian. These values were obtained from photomultiplier currents, the ultraviolet portion of the signal having been attenuated 50 per cent in passing through a Corning ultraviolet filter. Moreover, the portion of this phototube current from 2537 A radiation varied between 30 per cent and 90 per cent. I shall use the worst of these figures, and assume that half of the intensity is in the σ^+ component, and take as an estimate 0.3 mw of 2537 A σ^+ radiation per square centimeter per steradian for the intensity of the pancake-shaped lamp that will be used in this experiment. Then

$$\phi_L = 3.8 \times 10^{14} \text{ photons/cm}^2\text{-steradian-sec} \tag{22}$$

With the present values, A = 40 cm^2 and d = 50 cm, substituted in Eq. 15, the number of 2537 A σ^+ photons per cm^2 per second going into the cell is

$$\phi_c = \frac{\phi_L A}{d^2} = 6 \times 10^{12} \text{ photons/cm}^2\text{-sec} \tag{23}$$

An estimate of β can be made from the width, $\Delta\nu_1$, of the rf resonance. If all other causes of broadening are eliminated, the minimum width of this rf resonance will be determined by the mean lifetime of an oriented Hg^{199} atom, τ_R.

$$\Delta\nu_1 \geq \frac{1}{2\pi\tau_R} = \frac{\beta}{\pi\tau_w} + \frac{1}{2\pi\tau_c} \tag{24}$$

Under the assumption that the wall-collision term is dominant,

$$\beta \leq \pi\tau_w\Delta\nu_1 = \frac{a\Delta\nu_1}{5.610} \tag{25}$$

Brossel (5, 7) reports that in his 4-cm cells this width is much less than 1 cycle,

Table VI-2. Summary of time constants and ground sublevel population ratio for optical pumping (theoretical).

	General Expression (for ^1S_o atom with $I = \frac{1}{2}$)	For Hg^{199} at 20°C with 2537 A σ^+ Radiation	For a = 2.86 cm; $\beta = 1/14,000$; $f = 1/16,000$; $\phi_c = 6 \times 10^{12}$ (photons/sec-cm^2)
τ_A	$\frac{1}{2\pi}\left(\frac{8NkT}{\pi M}\right)^{1/2} \frac{d^2}{\phi_L A} \frac{\tau}{\lambda^3}$	$5.04 \times 10^{12} \frac{d^2}{\phi_L A}$	0.84 sec
τ_w	$a\left(\frac{\pi M}{8NkT}\right)^{1/2}$	$5.665 \times 10^{-5}\ a$	1.62×10^{-4} sec
τ_c	$\frac{6a}{f}\left(\frac{\pi M}{8NkT}\right)^{1/2}$	$3.40 \times 10^{-4} \frac{a}{f}$	15.6 sec
τ_P	$\frac{a\left(\frac{\pi M}{32NkT}\right)^{1/2}}{\frac{a}{2}\left[\frac{\pi^2}{12}\frac{M}{NkT}\frac{\phi_L A}{d^2}\frac{\lambda^3}{\tau}\right] + (\beta + f/12)}$	$\frac{2.83 \times 10^{-5}\ a}{1.87 \times 10^{-18}\ a \frac{\phi_L A}{d^2} + (\beta + f/12)}$	0.74 sec
τ_R	$\left(\frac{\pi M}{32NkT}\right)^{1/2} \frac{a}{\beta + f/12}$	$2.83 \times 10^{-5} \frac{a}{\beta + f/12}$	1.06 sec
α	$1 + \left[\frac{\pi^2}{12}\frac{M}{NkT}\frac{\phi_L A}{d^2}\frac{\lambda^3}{\tau}\right]\frac{a}{\beta + f/12}$	$1 + 3.75 \times 10^{-18} \frac{\phi_L A}{d^2} \frac{a}{\beta + f/12}$	1.84

Note: $\phi_c = (\phi_L A)/d^2$.

probably 1/10 of a cycle. Then $\beta \leq 1/14,000$.

In view of condition (d), the cell should be designed so that $f \leq 1/14,000$. The new cell was constructed with a = 9/8 inch = 2.86 cm, and with the hole connecting the cell to the tail of 0.01 inch diameter. Then $f = 1/16,000$.

With these estimates of ϕ_c, β, and f the time constants and population ratio for the Hg^{199} optical-pumping experiments can now be calculated. They are given in Table VI-2.

7. Conclusion

Table VI-2 summarizes the results of this report. The general expressions for the optical-pumping time constants and the ground sublevel population ratio are applicable to any atom whose ground-level configuration is ^1S_o and whose nucleus has spin I = 1/2, provided that the pumping is done through an F = 1/2 excited level. Some of these isotopes are He^3, Pd^{111}, Cd^{111}, Cd^{113}, Xe^{129}, Hg^{197}, and Hg^{199}.

Table VI-3. Comparison of optical pumping in $I = \frac{1}{2}$ and $I = \frac{3}{2}$ ^1S_o atoms.

	^1S_o $I = \frac{1}{2}$	^1S_o $I = \frac{3}{2}$	Effect of Approximation on I = 3/2 Values
τ_P	$\dfrac{1}{\frac{1}{3\tau_A} + \frac{2\beta}{\tau_w} + \frac{1}{\tau_c}}$	$\dfrac{1}{\frac{1}{3\tau_A} + \frac{4\beta}{3\tau_w} + \frac{1}{\tau_c}}$	Maximum Error = +1.62 per cent for $\tau_A = 0$
τ_R	$\dfrac{1}{\frac{2\beta}{\tau_w} + \frac{1}{\tau_c}}$	$\dfrac{1}{\frac{4\beta}{3\tau_w} + \frac{1}{\tau_c}}$	None
a	$1 + \dfrac{1}{3\tau_A\left(\frac{\beta}{\tau_w} + \frac{1}{2\tau_c}\right)}$	$1 + \dfrac{1}{\tau_A\left(\frac{\beta}{\tau_w} + \frac{3}{4\tau_c}\right)}$	Maximum Error = -0.36 per cent for $\tau_A = 0.35\ \tau_R$

The particular results for Hg^{199} indicate that 30 per cent optical pumping is expected, which produces a ground sublevel population ratio of 1.84 to 1. The expected mean pumping time is 0.74 sec, and the expected mean relaxation time is 1.06 sec. Optical pumping has recently been achieved in Hg^{199}. The measured ground sublevel population ratio is 2.0 to 1, and the experimental mean pumping time is 2.7 ± 0.6 sec.

Extension of this theory to ^1S_o atoms with higher nuclear spins is straightforward, and leads to a coupled set of 2I first-order linear differential equations, subject to the condition that the sum of all 2I + 1 ground sublevel populations equals the total number

of atoms, n_o. The solution for the population of the m = +I ground sublevel, when pumping is done through an excited F = I level, will, in general, be equal to a constant plus a sum of 2I different exponential terms. Even for I = 3/2, this solution is quite involved. However, the time constants and the upper-to-lower ground sublevel ratio for the I = 3/2 case can be approximated to a surprisingly good extent by expressions that are quite similar to those derived for I = 1/2. The error resulting from these approximations is never large enough to be experimentally detectable. Comparison of the I = 3/2 with the I = 1/2 results is made in Table VI-3. The net effect on the population ratio of the upper-to-lower ground sublevels (m = +3/2 to m = -3/2 of I = 3/2 compared with m = +1/2 to m = -1/2 of I = 1/2) is to give virtually the same effect as tripling the light intensity. However, this does not necessarily indicate that three times as much optical pumping can be obtained (for example, for Hg^{201} compared with Hg^{199}). The disorienting fraction of wall collisions, β, may also increase because of the effect of the nuclear electric quadrupole moment upon collisions.

With the introduction of the nuclear spin I, Eqs. 1-11 can now be generalized to hold for both I = 1/2 and I = 3/2. It remains to be determined whether they will also hold for I > 3/2. In summary,

$$\alpha = 1 + \frac{1}{3\tau_A\left(\frac{1}{2I}\,\frac{\beta}{\tau_w} + \frac{1}{2I+1}\,\frac{1}{\tau_c}\right)} \tag{26}$$

$$\alpha = (2I+1)\,\frac{\tau_R}{\tau_P} - 2I \tag{27}$$

$$\tau_P = \frac{3\tau_A\tau_R}{3\tau_A + \tau_R} = \frac{2I+1}{2I+\alpha}\,\tau_R \tag{28}$$

$$\tau_R = \frac{2I+\alpha}{2I+1}\,\tau_P = \frac{1}{\frac{2I+1}{2I}\,\frac{\beta}{\tau_w} + \frac{1}{\tau_c}} \tag{29}$$

$$\tau_A = \frac{\tau_P\tau_R}{3(\tau_R - \tau_P)} = \frac{\alpha + 2I}{\alpha - 1}\,\frac{\tau_P}{3} \tag{30}$$

$$\beta = \frac{2I}{2I+1}\,\tau_w\left(\frac{1}{\tau_R} - \frac{1}{\tau_c}\right) \tag{31}$$

The general pumping equation is

$$n = \frac{n_o}{2I+\alpha}\left[\alpha - \left(\alpha - \frac{2I+\alpha}{2I+1}\right)e^{-t/\tau_P}\right] \tag{32}$$

The general relaxation equation is

$$n = \frac{n_o}{2I+1}\left[1+\left(\frac{2I+1}{2I+a}\,a-1\right)e^{-t/\tau_R}\right] \tag{33}$$

W. T. Walter

References

1. J. Brossel and F. Bitter, Phys. Rev. 86, 308 (1952).
2. F. Boutron, J. P. Barrat, and J. Brossel, Compt. rend. 245, 2250 (1957).
3. W. Franzen, Phys. Rev. 115, 850 (1959).
4. F. Bitter, Nuclear Physics (Addison-Wesley Press, Cambridge, Mass., 1950), p. 56.
5. J. Brossel, private communication, Massachusetts Institute of Technology, September 1959.
6. A. C. Melissinos, Quarterly Progress Report, Research Laboratory of Electronics, M.I.T., Jan. 15, 1956, p. 36.
7. B. Cagnac and J. Brossel, Compt. rend. 249, 77 (1959).